

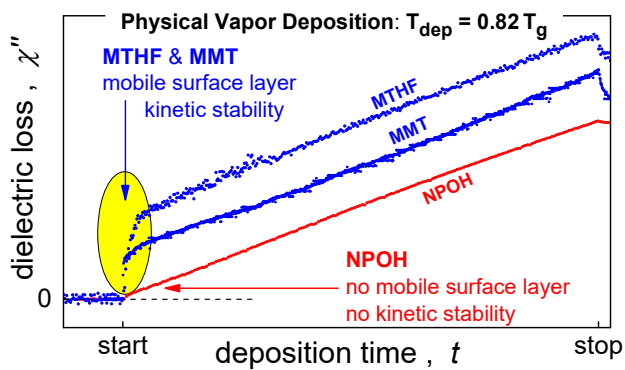
Dielectric study of n-propanol during physical vapor deposition: No surface mobility - no kinetic stability

R. Richert *

School of Molecular Sciences, Arizona State University, Tempe, Arizona 85287, USA

Abstract: Dielectric relaxation experiments have been performed on *n*-propanol (NPOH) films during physical vapor deposition at temperatures above and below its glass transition, $T_g = 97$ K. The results for NPOH are compared with those of analogous experiments on methyl-*m*-toluate (MMT) and 2-methyltetrahydrofuran (MTHF), with all three deposited at the same reduced temperature, $0.82T_g$. While MMT and MTHF display clear signs of a highly mobile surface layer, no such feature is observed for NPOH. The existence of this *in-situ* observed mobile surface layer correlates perfectly with the material's ability to form kinetically stable glasses, as NPOH differs from MMT and MTHF by not displaying kinetic stability.

Keywords: physical vapor deposition, dielectric properties, glass transition, thin films.



TOC Graph

■ INTRODUCTION

Molecular glasses prepared by physical vapor deposition (PVD) can display higher kinetic stability, higher density, lower energy and elevated anisotropy relative to glasses obtained by cooling the melt and subsequent physical aging.^{1,2} For a number of molecular glass formers, vapor deposition at a low rate and a substrate temperature near $0.85T_g$ yield states much closer to equilibrium than achievable by cooling the melt and extended physical aging at the same temperature.^{3,4} The common understanding of the origin of such high kinetic stability rests on the combination of a low temperature (as thermodynamic driving force towards high packing density) and a high mobility within a surface layer (facilitating fast sampling of phase space),⁵ a situation that does not occur in bulk samples. Such a surface mediated kinetic stability is supported by simulations of vapor deposition scenarios.^{6,7}

An increased diffusivity at the vacuum interface or surface of molecular glasses is a common feature, and has been observed for a variety of liquid quenched glasses.^{8,9,10,11} Surface measurements on films that had been prepared by vapor deposition display a similar enhancement of mobility by orders of magnitude relative to that in the bulk.^{12,13} Recently, measurements of the dielectric relaxation of films during physical vapor deposition have been reported.^{14,15} These experiments have observed enhanced surface dynamics associated with molecular reorientation for methyl-*m*-toluate (MMT, $T_g = 170$ K)¹⁴ and 2-methyltetrahydrofuran (MTHF, $T_g = 91$ K)¹⁵. Both MTHF and MMT are known to display high kinetic stability when subject to PVD at a deposition temperature around $T_{dep} = 0.82T_g$ and at a moderate deposition rate r_{dep} .¹⁶ In the case of MTHF, the level of kinetic stability has been inferred not only from an increased onset temperature,¹⁷ but also from the PVD induced suppression of its β -relaxation,¹⁸ a feature that is found to correlate with kinetic stability.¹⁶

Not all molecular glass formers are capable of becoming glasses of high kinetic stability when vapor deposited at conditions that lead to kinetic stability for many other systems, i.e., $0.8T_g \leq T_{dep} \leq 0.9T_g$ and $r_{dep} < 0.5$ nm/s. This has been documented by the observation of a wide range of kinetic stabilities for alcohol glasses.^{19,20} Among these alcohols, *n*-propanol (NPOH) stands out as resisting to reach a kinetically stable state for a variety of deposition conditions which lead to highly stable glasses for other molecular materials.¹⁹ For the case of 2-ethyl-1-hexanol, it has been indicated that the absence of considerable surface mobility can be a key factor in inhibiting the

formation of a highly stable glass.²⁰ In support of this notion, hydrogen-bonding has been reported to slow down surface mobility.²¹

By virtue of the lack of kinetic stability of vapor deposited NPOH, this monohydric alcohol facilitates addressing the question whether the observation of a surface layer with fast reorientational dynamics (high dielectric loss) during deposition is actually correlated with the formation of a glass with high kinetic stability. To answer this question, films of NPOH have been vapor deposited under conditions that fail to generate stable glasses of NPOH, but do lead to kinetic stability for MTHF and MMT. It is found that high resolution dielectric measurements on NPOH during vapor deposition provide no indication of a surface layer with enhanced dynamics, in qualitative contrast to the cases of MTHF and MMT. Therefore, the mobile surface layer observed by dielectric techniques from beginning to end of the deposition process is directly linked to the kinetic stability of the glass formed below. It is also observed that the bulk of the vapor deposited NPOH film is subject to aging, consistent with the absence of kinetic stability, and that even above T_g the equilibrium hydrogen-bonded structures are established only slowly.

■ EXPERIMENT

The sample material *n*-propanol (NPOH, 99.7%, anhydrous) has been purchased from Sigma-Aldrich and was used as received. NPOH was vapor deposited onto a substrate that was cooled using a Leybold RDK 12-320 closed-cycle helium refrigerator within a vacuum chamber, and temperature was controlled with a Lakeshore Mod. 340 unit. A reservoir (≈ 1 L) of NPOH vapor was kept at a pressure of 1 mbar, and the deposition rates and times were adjusted by a needle valve and toggle valves, respectively. Details of the deposition chamber have been provided in a previous publication.²² Samples were deposited onto a microlithographically fabricated interdigitated electrode (IDE) cell, ABTECH IME 1050.5-FD-Au, with borosilicate substrate.²³ The capacitor structure consists of $n/2 = 50$ pairs of 100 nm thick gold fingers ($l = 5$ mm length, $w = 10$ μ m width, and $s = 10$ μ m digit spacing). The nominal geometric capacitance of $C_{geo} = \epsilon_0 \times L/2 = 2.2$ pF has been verified, where $L = (s + w + l) \times (n - 1) = 49.55$ cm is the serpentine length of the structure and ϵ_0 is the permittivity of vacuum. The periodicity of this structure is $\lambda = 2(s + w) = 40$ μ m, and the electric field extends $\lambda/2 = 20$ μ m normal to the substrate.²⁴

For the present vapor deposited films, the IDE capacitor is not completely filled along the z -axis, implying that the measured susceptibility χ_{app} remains a filling factor of γ below the actual susceptibility χ of the material. For films thicknesses up to $d = 500$ nm, χ_{app} increase linearly with d , where $\chi_{app} = \chi \times d/(\lambda/8)$. Film thicknesses are determined by depositing films at several temperatures at which the dielectric permittivity at 1 kHz is near the high frequency limit ϵ_∞ and then comparing with the respective values for bulk NPOH.

The capacitance, C , and dissipation, $D = \tan\delta$, have been measured during and after deposition onto the IDE using an ultraprecision capacitance bridge Andeen-Hagerling AH-2700A set to a fixed frequency $\nu = 1$ kHz. In the glassy state, the real part of the capacitance, C' , is governed by ϵ_∞ and thus a reliable indicator of film thickness. The imaginary part, C'' , reflects residual dynamics of the glass and thus its fictive temperature. The time dependent apparent susceptibility, χ_{app} , of the sample is determined using the relations

$$\chi'_{app}(t) = [C'(t) - C'_{sub}]/C_{geo}, \quad (1a)$$

$$\chi''_{app}(t) = [C''(t) - C''_{sub}]/C_{geo}, \quad (1b)$$

where $C' = C$, $C'' = C \times \tan\delta$, and C_{sub} represents the capacitance value prior to deposition, which is governed by the borosilicate substrate. The subscript 'app' denotes the apparent value of the susceptibility, which is the real value χ multiplied by a filling factor $\gamma = d/(\lambda/8)$ that depends on the film thickness d , for $d \leq 500$ nm, and thus also on time, t , during the course of the deposition process with constant rate $r_{dep} = \partial d/\partial t$. After deposition, the film thickness is determined via

$$d_{dep} = \frac{\lambda}{8} \times \frac{\Delta\chi'_{app}}{\chi'} = 5 \text{ } \mu\text{m} \times (\Delta\chi'_{app}/\chi'), \quad (2)$$

where $\Delta\chi'_{app}$ is the total increment of χ'_{app} accumulated during deposition and χ' is a calibration value obtained from a bulk sample of NPOH. The average deposition rate is given by $r_{dep} = d_{dep}/t_{dep}$, with t_{dep} being the duration of the deposition. Spectra of the sample in the liquid state are collected *in-situ* using a Solartron SI-1260, equipped with a calibrated DM-1360 transimpedance amplifier.

■ RESULTS

The result of vapor depositing NPOH at a constant deposition rate r_{dep} onto the IDE substrate held at $T_{dep} = 80$ K is shown in Figure 1 in terms of $\chi'_{app}(t)$ and $\chi''_{app}(t)$. The index 'app' implies

that the ordinate scale values reflect the incomplete filling of the capacitor, but absolute values are not relevant at this point. The main feature of this result is that both $\chi'_{\text{app}}(t)$ and $\chi''_{\text{app}}(t)$ rise linearly with time, i.e., near perfect proportionality, $\chi''_{\text{app}}(t) \propto \chi'_{\text{app}}(t)$, is preserved for the entire duration of the deposition, $t_{\text{dep}} = 1000$ s. As discussed below, such a proportionality is not observed with other molecules. Another observation is that $\chi''_{\text{app}}(t)$ decreases after deposition had stopped, whereas $\chi'_{\text{app}}(t)$ remains practically constant for $t > t_{\text{dep}}$.

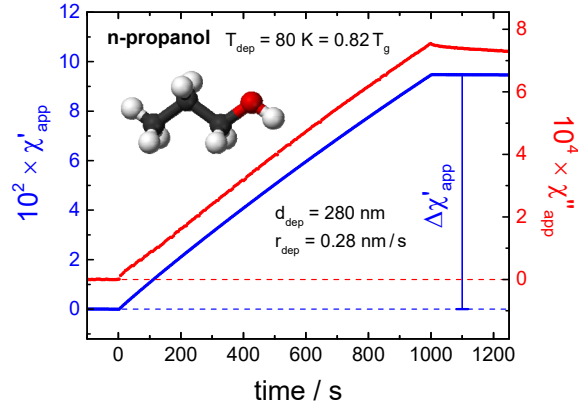


Figure 1. Apparent susceptibilities, χ'_{app} and χ''_{app} at $\nu = 1$ kHz, versus time of an NPOH film during deposition at $T_{\text{dep}} = 80$ K for a time $t_{\text{dep}} = 1000$ s at a rate $r_{\text{dep}} = 0.28$ nm/s, leading to a film of thickness $d_{\text{dep}} = 280$ nm. The value of χ'_{app} is highly stable after deposition, whereas χ''_{app} decreases for $t > 1000$ s. The real part of permittivity increased by $\chi'_{\text{app}}(t = 1000 \text{ s}) = \Delta\chi'_{\text{app}} = 0.095$.

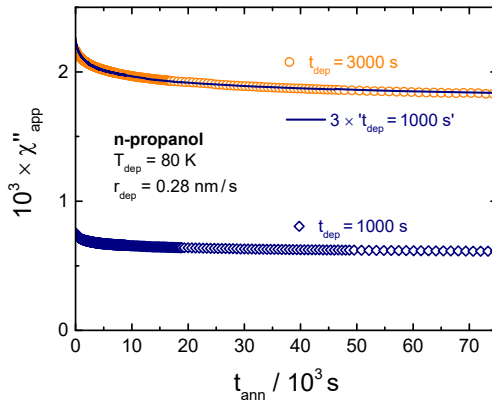


Figure 2. Annealing effect on the dielectric loss, χ''_{app} , at $\nu = 1$ kHz versus annealing time t_{ann} , the time after deposition had stopped. Data are shown for two films, both deposited at $T_{\text{dep}} = 80$ K with a rate $r_{\text{dep}} = 0.28$ nm/s, one deposited for $t_{\text{dep}} = 1000$ s (diamonds) and the other for 3000 s (circles). The line represents the $t_{\text{dep}} = 1000$ s case but scaled up a factor of 3, the thickness ratio of the two films.

Another film of NPOH has been deposited at $T_{\text{dep}} = 80$ K and $r_{\text{dep}} = 0.28$ nm/s, but this time for a duration of $t_{\text{dep}} = 3000$ s, leading to a film three times thicker than in the case of Figure 1. The

deposition behavior is analogous to that shown in Figure 1, again with $\chi''_{\text{app}}(t) \propto \chi'_{\text{app}}(t)$ for the 3000 s duration of the deposition. Figure 2 displays the annealing effects of the two films that differ only in their thicknesses, i.e., the reductions of $\chi''_{\text{app}}(t_{\text{age}})$ with time after deposition had stopped, where $t_{\text{age}} = t - t_{\text{dep}}$. The line in Figure 2 represents $3 \times \chi''_{\text{app}}(t_{\text{age}})$ of the thinner film, and it coincides with $\chi''_{\text{app}}(t_{\text{age}})$ of the thicker film, indicating that the bulk of the film is involved in this annealing effect.

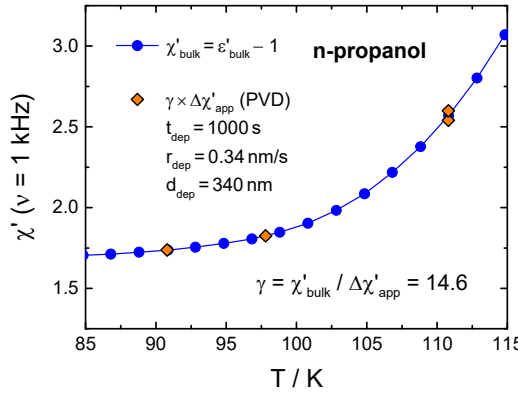


Figure 3. Dielectric susceptibilities at $\nu = 1$ kHz versus temperature for bulk NPOH (χ'_{bulk} , circles) and for four vapor deposited films with deposition temperatures $T_{\text{dep}} = 90.8, 97.8, 110.8$ and 110.8 K ($\gamma \times \Delta \chi'_{\text{app}}$, diamonds). All films were deposited for $t_{\text{dep}} = 1000$ s and at the same constant rate r_{dep} . The scaling parameter $\gamma = 14.6$ is identical for the four films, leading to film thicknesses of $d_{\text{dep}} = 5000$ nm/ $\gamma = 340$ nm and rates $r_{\text{dep}} = 0.34$ nm/s. Bulk NPOH data is taken from ref. 25.

A set of four more NPOH films have been deposited, all at a common deposition rate, $r_{\text{dep}} = 0.34$ nm/s, and for the same deposition time, $t_{\text{dep}} = 1000$ s, so that these films have a common thickness of 340 nm. The parameter in which these films differ is the deposition temperature, $T_{\text{dep}} = 90.8, 97.8, 110.8$ and 110.8 K. Qualitatively, the deposition curves for these temperatures match the $T_{\text{dep}} = 80$ K scenario of Figure 1, namely that the proportionality $\chi''_{\text{app}}(t) \propto \chi'_{\text{app}}(t)$ is again observed for the duration of the deposition. In the order of increasing T_{dep} , the permittivity increments during deposition are $\Delta \chi'_{\text{app}} = 0.119, 0.125, 0.174$, and 0.178 . These quantities are depicted as diamonds in Figure 3 after scaling up by a common factor γ . Based on a comparison with bulk NPOH,²⁵ it turns out that a factor of $\gamma = 14.6$ generates $\chi' = \gamma \times \Delta \chi'_{\text{app}}$ values that are consistent with those of bulk NPOH at the respective temperatures. This value of γ facilitates determining absolute values for the film thicknesses and deposition rates, as the real part of susceptibility, χ'_{app} , is insensitive to mobility and thus a robust measure of the amount of material.

The two results for $T_{\text{dep}} = 110.8$ K also demonstrate that the amplitudes $\Delta\chi'_{\text{app}}$ are well reproduced in subsequent deposition processes with nominally identical deposition parameters.

One of the films deposited at $T_{\text{dep}} = 110.8$ K has been subsequently subject to dielectric relaxation experiments across frequencies ranging from 0.1 Hz to 100 kHz for temperatures between 110 and 140 K. The results are shown in Figure 4 after scaling up with the factor γ derived from the data of Figure 3, so that the amplitudes can be compared with those of bulk NPOH. The key observation in Figure 4 is that the height of the low frequency plateau has increased from the first (dashed line) to the second (solid line) scan at 130 K. This implies that the static dielectric constant, ε_s , of the as-deposited film increases slowly by 25 % to near the value expected for the bulk equilibrium liquid.

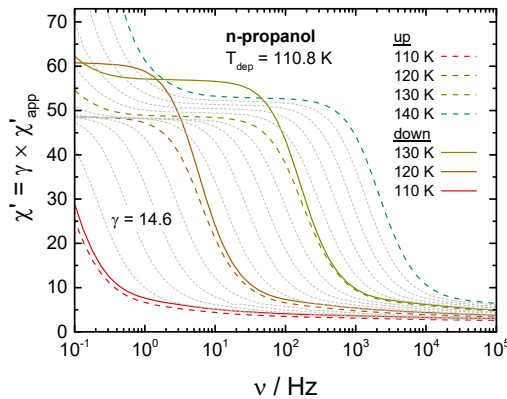


Figure 4. Scaled permittivity spectra, $\chi' = \gamma \times \chi'_{\text{app}}$ versus frequency ν , for an NPOH film deposited at $T_{\text{dep}} = 110.8$ K. Spectra are shown for various temperature increasing from 110 to 140 K (dashed lines) and decreasing again to 110 K (solid lines). The dotted lines display the intermediate spectra taken at 2 K steps for the 110 to 140 K sequence. Scaling by the factor γ taken from Figure 3 leads to an ordinate scale that is comparable to values for bulk NPOH.

■ DISCUSSION

High kinetic stability is the hallmark of films of many molecular materials when vapor deposited at a temperature somewhat below T_g and at a moderate rate. The signature of such stable glasses is a calorimetric onset temperature positioned well above the glass transition temperature, with T_g referring to a glass prepared by cooling the melt at about 20 K/min.⁴ Not all materials display high kinetic stability after vapor deposition using the parameters $0.80T_g \leq T_{\text{dep}} \leq 0.90T_g$ and $r_{\text{dep}} < 0.5$ nm/s.^{19,20} Following the concept of surface mediated kinetic stability, a mobile surface layer is required in order for molecules or atoms to sample phase space efficiently, so that states of low energy are found before becoming buried by subsequent deposition. Many simple

liquids do show enhanced surface mobility over that of the bulk, because the interactions impeding mobility are reduced considerably at a vacuum or gas interface.^{8,9,10,11,12,13,14,15}

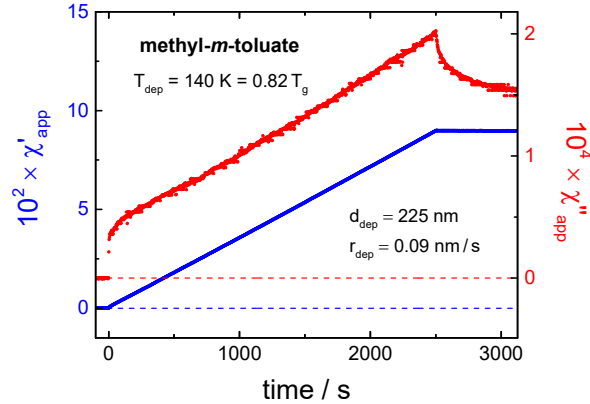


Figure 5. Apparent susceptibilities, χ'_{app} and χ''_{app} at $\nu = 1$ kHz, versus time of a methyl-m-toluate film during deposition at $T_{\text{dep}} = 140$ K for a time $t_{\text{dep}} = 2500$ s at a rate $r_{\text{dep}} = 0.09$ nm/s, leading to a film of thickness $d_{\text{dep}} = 225$ nm. Note the initial rapid increase of χ''_{app} , a feature that is absent in the case of NPOH. Data taken from ref. 14.

Both vapor deposited and melt-quenched glasses display surface diffusivities that are orders of magnitude above those of the bulk counterpart.^{8,9,10,11} However, in order to achieve high kinetic stability by PVD, the surface mobility needs to be high for the duration of the deposition process, not afterwards. Therefore, the focus of this work is to demonstrate the correlation between enhanced surface mobility observed during vapor deposition and high kinetic stability of the as deposited glass. The dielectric curves in Figure 1, $\chi'_{\text{app}}(t)$ and $\chi''_{\text{app}}(t)$, may appear unsurprising and not very informative, as both real and imaginary components of susceptibility rise linearly with time and thus with film thickness. The important aspect of the proportionality $\chi''_{\text{app}}(t) \propto \chi'_{\text{app}}(t)$ observed for all temperatures (80 - 110.8 K, $0.82T_g$ - $1.14T_g$) as in Figure 1 becomes clear when comparing with analogous results obtained for two other materials: MMT shown in Figure 5 and MTHF shown in Figure 6. Both MMT and MTHF have been deposited at similar conditions relative to their T_g , i.e., $T_{\text{dep}} = 0.82T_g$, and both display an initial fast rise of $\chi''_{\text{app}}(t)$, even though the constant slope of $\chi'_{\text{app}}(t)$ indicates a time-invariant deposition rate. The initial higher slope of $\chi''_{\text{app}}(t)$ is a clear indication of enhanced surface mobility, in both cases the equivalent of a liquid with fictive temperature above T_g .¹⁴ Details on the surface dynamics of MMT and MTHF can be found in the original publications.^{14,15} Clearly, such an initial rapid rise of $\chi''_{\text{app}}(t)$ is absent in the case of NPOH, cf. Figure 1. The occurrence of the high surface mobility observed as enhanced

initial $\chi''_{\text{app}}(t)$ slope correlates perfectly with the ability of the material to form kinetically highly stable glasses. Vapor deposited glasses of both MMT and MTHF have been observed to form kinetically stable states when deposited at $T_{\text{dep}} = 0.82T_g$ and at a moderate deposition rate, $r_{\text{dep}} < 0.5 \text{ nm/s}$.¹⁶ By contrast, NPOH has not shown signs of enhanced stability when vapor deposited under similar conditions.¹⁹

Comparing the $\chi''_{\text{app}}(t)$ curves in Figure 1, Figure 5, and Figure 6, one can also observe that $\chi''_{\text{app}}(t)$ decreases with time in all three cases after deposition had terminated. For both MMT and MTHF, this aging process has been clearly recognized to occur within the mobile surface layer, as it is independent of film thickness.^{14,15} This notion is consistent with the high kinetic stability of the bulk of the glasses below, as their states prohibit aging on laboratory time scales. NPOH differs in this respect as well, as the amplitude of the aging response scales with the sample thickness, cf. Figure 2, indicating that this annealing effect occurs within the entire volume of the NPOH film. This feature is consistent with the low kinetic stability of NPOH, similar to that of the melt-quenched counterpart. Low stability allows for the bulk of the film to age within the present observation time window, whereas a material with high kinetic stability is not expected to display aging for at least 1000 years.⁴

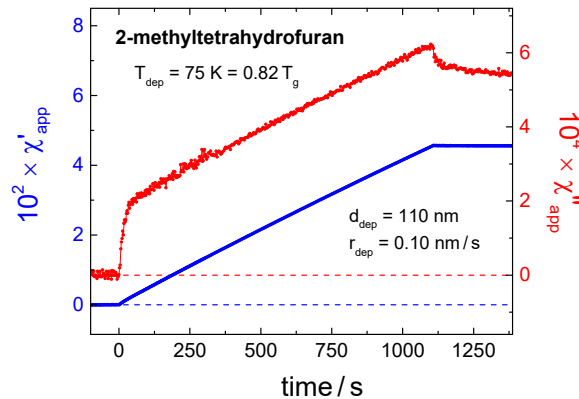


Figure 6. Apparent susceptibilities, χ'_{app} and χ''_{app} at $\nu = 1 \text{ kHz}$, versus time of a 2-methyltetrahydrofuran film during deposition at $T_{\text{dep}} = 75 \text{ K}$ for a time $t_{\text{dep}} = 1110 \text{ s}$ at a rate $r_{\text{dep}} = 0.10 \text{ nm/s}$, leading to a film of thickness $d_{\text{dep}} = 110 \text{ nm}$. Note the initial rapid increase of χ''_{app} , a feature that is absent in the case of NPOH. Data taken from ref. 15.

In the present context, the critical difference between NPOH and the other two molecules is the hydroxyl group of NPOH, which facilitates hydrogen-bonding among the molecules, see inset of Figure 1. By contrast, both MMT and MTHF are van-der-Waals type glass formers. As in the

case of 2-ethyl-1-hexanol²⁰ and other monohydric alcohols,¹⁹ hydrogen bonding is assumed responsible for the lack of considerable surface mobility of NPOH. When cooling bulk NPOH from the melt, this alcohol forms chain-like supramolecular structures, as evident from its high Kirkwood correlation factor $g_K \approx 4$ in the supercooled state.²⁶ These hydrogen-bonded chains and the subsequent more parallel configuration of neighboring dipoles are responsible for the high dielectric constant, $\epsilon_s \approx 70$, of NPOH at $T = 120$ K.²⁵ Figure 4 demonstrates that a film deposited at $T_{dep} = 110$ K ($= T_g + 13$ K) does not reach the equilibrium static dielectric constant of NPOH quickly. Apparently, establishing the equilibrium supramolecular structure remains slow even at $T = 140$ K. In the course of the 5 hour data acquisition leading to the results of Figure 4, the dielectric constant increased from $\epsilon_s = 48$ to 61 at $T = 120$ K. Within the uncertainty of the scaling factor γ , the final value of 61 may correspond to the equilibrium ϵ_s of bulk NPOH.

It has been observed before that vapor deposited films of monohydric alcohols tend to display a Kirkwood correlation factor closer to $g_K = 1$ after warming to above T_g . In the case of 4-methyl-3-heptanol (4M3H), the permittivity dropped considerably while warming the as-deposited film.²⁷ The alcohol 4M3H has a strong tendency to form hydrogen bonded rings rather than chains, leading to dipole moment cancellation and a correlation factor $g_K \approx 0.1$.²⁸ Both cases, NPOH and 4M3H are consistent with vapor deposited films preferring a more random structure with an orientational correlation closer to $g_K = 1$. Unity regarding g_K indicates the lack of orientational correlation regarding neighboring dipoles, which would stem from the inability to establish the equilibrium supramolecular structures, chain- or ring-like, during vapor deposition.

■ SUMMARY AND CONCLUSIONS

The dielectric properties of *n*-propanol films have been recorded during vapor deposition at temperatures ranging from 80 K to 110.8 K ($0.82T_g$ to $1.14T_g$). The proportionality between $\chi''(t)$ and $\chi'(t)$ observed for all temperatures indicates the lack of a mobile surface layer, whose signature would be a rapid initial rise of the dielectric loss $\chi''(t)$ relative to that of $\chi'(t)$. Such signatures of a mobile surface layer have been documented for MMT and MTHF, and both materials form glasses of high kinetic stability under comparable deposition conditions, $T_{dep} = 0.82T_g$ and $r_{dep} < 0.5$ nm/s. From the fact that NPOH fails to achieve enhanced stability at similar deposition conditions, we conclude that a surface layer associated with high dielectric loss and thus high rotational mobility is a prerequisite for the formation of glasses with high kinetic stability. Therefore, an *in-situ*

dielectric characterization of vapor deposited films can reveal not only the growth process but also whether kinetic stability and other extraordinary properties may be expected for the deposition conditions used.

Hydrogen bonding in NPOH is not only the likely cause for the lack of enhanced surface mobility, but also responsible for the low dielectric constant, ϵ_s , of vapor deposited NPOH relative to its counterpart cooled from the melt. Observing that ϵ_s increases slowly after warming an as-deposited glass to above T_g is seen as indicator of NPOH's inability to achieve the equilibrium hydrogen-bonded supramolecular structures during deposition, even when deposited at $T_g + 13$ K. These chain-like structures lead to a high Kirkwood correlation factor g_K , which in turn is responsible for the high dielectric constant of this monohydric alcohol relative to its dipole density.

■ ACKNOWLEDGMENTS

This work was supported by the National Science Foundation under Grant No. CHE-2153944.

■ AUTHOR INFORMATION

Corresponding Author

Ranko Richert – *School of Molecular Sciences, Arizona State University, Tempe, Arizona 85287, USA*;

 orcid.org/0000-0001-8503-3175; Email: ranko@asu.edu

Notes

The authors declare no competing financial interest.

■ REFERENCES

- (1) Swallen, S. F.; Kearns, K. L.; Mapes, M. K.; Kim, Y. S.; McMahon, R. J.; Ediger, M. D.; Wu, T.; Yu, L.; Satija, S. Organic glasses with exceptional thermodynamic and kinetic stability. *Science* **2007**, *315*, 353-356.
- (2) Berthier, L.; Ediger, M. D. Facets of glass physics. *Phys. Today* **2016**, *69*, 40-46.
- (3) Beasley, M. S.; Bishop, C.; Kasting, B. J.; Ediger, M. D. Vapor-deposited ethylbenzene glasses approach "ideal glass" density. *J. Phys. Chem. Lett.* **2019**, *10*, 4069-4075.

(4) Ediger, M. D. Perspective: Highly stable vapor-deposited glasses. *J. Chem. Phys.* **2017**, *147*, 210901.

(5) Luo, P.; Fakhraai, Z. Surface-mediated formation of stable glasses. *Annu. Rev. Phys. Chem.* **2023**, *74*, 361-389.

(6) Singh, S.; de Pablo, J. J. A molecular view of vapor deposited glasses. *J. Chem. Phys.* **2011**, *134*, 194903.

(7) Berthier, L.; Charbonneau, P.; Flenner, E.; Zamponi, F. Origin of ultrastability in vapor-deposited glasses. *Phys. Rev. Lett.* **2017**, *119*, 188002.

(8) Brian, C. W.; Yu, L. Surface self-diffusion of organic glasses. *J. Phys. Chem. A* **2013**, *117*, 13303-13309.

(9) Yu, L. Surface mobility of molecular glasses and its importance in physical stability. *Adv. Drug Deliv. Rev.* **2016**, *100*, 3-9.

(10) Zhang, Y.; Fakhraai, Z. Decoupling of surface diffusion and relaxation dynamics of molecular glasses. *Proc. Natl. Acad. Sci. U. S. A.* **2017**, *114*, 4915-4919.

(11) Li, Y.; Zhang, W.; Bishop, C.; Huang, C.; Ediger, M. D.; Yu, L. Surface diffusion in glasses of rod-like molecules posaconazole and itraconazole: effect of interfacial molecular alignment and bulk penetration. *Soft Matter* **2020**, *16*, 5062-5070.

(12) Samanta, S.; Huang, G.; Gao, G.; Zhang, Y.; Zhang, A.; Wolf, S.; Woods, C. N.; Jin, Y.; Walsh, P. J.; Fakhraai, Z. Exploring the importance of surface diffusion in stability of vapor-deposited organic glasses. *J. Phys. Chem. B* **2019**, *123*, 4108-4117.

(13) Zhang, Y.; Potter, R.; Zhang, W.; Fakhraai, Z. Using tobacco mosaic virus to probe enhanced surface diffusion of molecular glasses. *Soft Matter* **2016**, *12*, 9115-9120.

(14) Richert, R.; Tracy, M. E.; Guiseppi-Elie, A.; Ediger, M. D. Anatomy of the dielectric behavior of methyl-m-toluate during and after vapor deposition. *J. Chem. Phys.* **2024**, *160*, 034505.

(15) Thoms, E.; Gabriel, J. P.; Guiseppi-Elie, A.; Ediger, M. D.; Richert, R. In-situ observation of fast surface dynamics during the vapor-deposition of a stable organic glass. *Soft Matter* **2020**, *16*, 10860-10864.

(16) Kasting, B. J.; Beasley, M. S.; Guiseppi-Elie, A.; Richert, R.; Ediger, M. D. Relationship between aged and vapor-deposited organic glasses: secondary relaxations in methyl-m-toluate. *J. Chem. Phys.* **2019**, *151*, 144502.

(17) Riechers, B.; Guiseppi-Elie, A.; Ediger, M. D.; Richert, R. Ultrastable and polyamorphic states of vapor-deposited 2-methyltetrahydrofuran. *J. Chem. Phys.* **2019**, *150*, 214502.

(18) Yu, H.-B.; Tylinski, M.; Guiseppi-Elie, A.; Ediger, M. D.; Richert, R. Suppression of β relaxation in vapor-deposited ultrastable glasses. *Phys. Rev. Lett.* **2015**, *115*, 185501.

(19) Tylinski, M.; Chua, Y. Z.; Beasley, M. S.; Schick, C.; Ediger, M. D. Vapor-deposited alcohol glasses reveal a wide range of kinetic stability. *J. Chem. Phys.* **2016**, *145*, 174506.

(20) Tylinski, M.; Beasley, M. S.; Chua, Y. Z.; Schick, C.; Ediger, M. D. Limited surface mobility inhibits stable glass formation for 2-ethyl-1-hexanol. *J. Chem. Phys.* **2017**, *146*, 203317.

(21) Chen, Y.; Zhang, W.; Yu, L. Hydrogen bonding slows down surface diffusion of molecular glasses. *J. Phys. Chem. B* **2016**, *120*, 8007-8015.

(22) Riechers, B.; Guiseppi-Elie, A.; Ediger, M. D.; Richert, R. Ultrastable and polyamorphic states of vapor-deposited 2-methyltetrahydrofuran. *J. Chem. Phys.* **2019**, *150*, 214502.

(23) Yang, L.; Guiseppi-Wilson, A.; Guiseppi-Elie, A. Design considerations in the use of interdigitated microsensor electrode arrays (IMEs) for impedimetric characterization of biomimetic hydrogels. *Biomed. Microdevices* **2011**, *13*, 279-289.

(24) Olthuis, W.; Streekstra, W.; Berveld, P. Theoretical and experimental determination of cell constants of planar-interdigitated electrolyte conductivity sensors. *Sensors and Actuators B: Chemical* **1995**, *24*, 252-256.

(25) Hansen, C.; Stickel, F.; Berger, T.; Richert, R.; Fischer, E. W. Dynamics of glass-forming liquids. III. Comparing the dielectric α - and β -relaxation of 1-propanol and o-terphenyl. *J. Chem. Phys.* **1997**, *107*, 1086-1093.

(26) Davidson, D. W.; Cole, R. H. Dielectric relaxation in glycerol, propylene glycol, and *n*-propanol. *J. Chem. Phys.* **1951**, *19*, 1484-1490.

(27) Young-Gonzales, A. R.; Guiseppi-Elie, A.; Ediger, M. D.; Richert, R. Modifying hydrogen-bonded structures by physical vapor deposition: 4-methyl-3-heptanol. *J. Chem. Phys.* **2017**, *147*, 194504.

(28) Dannhauser, W. Dielectric study of intermolecular association in isomeric octyl alcohols. *J. Chem. Phys.* **1968**, *48*, 1911-1917.